Front. Phys. 13(1), 136103 (2018)
https://doi.org/10.1007/s11467-017-0714-6

REVIEW ARTICLE

Fragile to strong crossover and Widom line in supercooled water: A comparative study

Margherita De Marzio, Gaia Camisasca, Mauro Rovere, Paola Gallo[†]

Dipartimento di Matematica e Fisica, Università Roma Tre, Italia
Corresponding author. E-mail: [†]*gallop@fis.uniroma3.it*
Received March 6, 2017; Accepted April 7, 2017

The aim of this paper is to discuss the relationship between the dynamics and thermodynamics of water in the supercooled region. Reviewed case studies comprehend bulk water simulated with the SPC/E, TIP4P and TIP4P/2005 potentials, water at protein interfaces, and water in solution with electrolytes. Upon supercooling, the fragile to strong crossover in the α-relaxation of water is found to occur when the Widom line emanating from the liquid-liquid critical point is crossed. This appears to be a general characteristic of supercooled water, not depending on the applied interaction potential and/or different local environments.

Keywords molecular dynamics simulation, supercooled water, slow dynamics, hydration water, aqueous solutions

PACS numbers 61.10.Ja, 64.60.My, 61.20.-p, 64.70.Pf

1 Introduction

Water is one of the most abundant and, at the same time, anomalous compound in the world [1–5]. The study of the thermodynamic and dynamical properties of this liquid is important for several reasons. Water, indeed, has a primary role in the field of biology [6, 7] and in various technological processes [2, 8]. Moreover, water exhibits more than 60 anomalies compared to other liquids, whose origin is still a matter of debate [2–5, 9]. In particular, a locus of temperature of maximum density, called TMD, exists and marks the region of the phase diagram where density decreases upon cooling the system, which is different from the case of simple liquids. Furthermore, thermodynamic response functions, such as the isothermal compressibility and isobaric specific heat, increase anomalously when temperature is lowered isobarically, and they seem to be asymptotically diverging in the supercooled regime, in contrast with the monotonic behavior of normal liquids [10, 11]. Although several theoretical and experimental studies have been conducted to understand the peculiar behavior of water [1, 3, 5], the increase of the nucleation rate in the deep supercooled regime makes difficult the exploration of an entire thermodynamic region called the "no man's land" [12].

Several scenarios have been developed to explain the thermodynamic anomalies of water [1]. Among these, the Liquid–Liquid Critical Point (LLCP) scenario, formulated by Poole, Sciortino, Essmann, and Stanley [13] is able to explain both the increase of thermodynamic response functions and glassy water polyamorphism theoretically. Indeed, a large number of experimental works on the amorphous phase of water confirmed the existence of two distinct forms of glassy water, Low-Density Amorphous Ice (LDA) and High-Density Amorphous Ice (HDA) [12, 14]. Furthermore, a first-order-type phase transition has been observed between HDA and LDA [15–18].

The central idea of the LLCP hypothesis is that supercooled liquid water can exist in two different phases: the Low Density Liquid state (LDL) and High Density Liquid state (HDL). LDL is a supercooled liquid state that is more open and ordered and it exhibits a network of hydrogen bonds with a local tetrahedral order extending to the second coordination shell. In comparison, HDL has a more disordered hydrogen bond structure with a coordination number of $N_{OO} > 4$ and the tetrahedral order is limited to the first coordination shell. A first order phase transition between LDL and HDL occurs in the "no man's land" and ends in a second order LLCP. The HDA-LDA phase transition is the low-temperature and high-pressure section of the LDL-HDL coexistence line, whose

*Special Topic: Water and Water Systems (Eds. F. Mallamace, R. Car, and Limei Xu).

negative slope indicates that HDL is a more entropic phase compared to LDL. Hence, on one hand, the LLCP hypothesis is compatible with the LDA-HDA phase transition and, on the other hand, interprets the anomalous increase of thermodynamic response functions in terms of the increase and asymptotic divergence that occurs upon approaching the critical point. Evidence supporting the presence of the LLCP has been found both by computer simulations and experimental studies. In particular, Mishima and Stanley located the LLCP at approximately $T \sim 220$ K and $P \sim 100$ MPa [15].

Within the framework of the LLCP scenario, a line of maxima of the correlation length, defined as the Widom Line (WL), is expected to emanate from the LLCP, at which the correlation length diverges, into the one-phase region [19, 20]. This line can be considered as a signature of the existence of the LLCP, and marks the transition of the liquid from a high-temperature, more HDL-like region toward a low-temperature phase, where the structure and dynamics of the system are more LDL-like. Expressed as power of the correlation length close to the LLCP, thermodynamic response functions also show loci of maxima in the one-phase region, which should collapse onto the WL, close to the critical point. From this, it follows that these maxima can be used as a proxy for the WL [20–22].

Apart from the thermodynamic behavior of water in the mild and deep supercooled regime, the dynamical properties of this liquid have been investigated in the last years as well. In 1996, computer simulation studies on SPC/E supercooled bulk water [23, 24] show that water follows the Mode Coupling Theory (MCT) of glass-forming liquids [25, 26]. The agreement between MCT and supercooled water dynamics was further confirmed by other computational and experimental studies [27–35].

In particular, it has been experimentally demonstrated that in mild supercooling water, the structural relaxation time increases as a power law, as predicted by MCT [35]. Nevertheless, upon further cooling, the presence of activated processes, called hopping processes, causes the increasing trend of the relaxation time from the MCT to change from power law to an exponential Arrhenius law. This deviation is called Fragile to Strong Crossover (FSC) and is interpreted as a transition from a region, where water behaves as a fragile liquid, toward a state where diffusivity is typical to that of a strong liquid. The presence of FSC has been found by computer simulations of both bulk [20, 27, 36] and confined [31, 32] water, and by experimental measurements of confined water [37–42] and more recently in layered ice/water samples [43]. The role of FSC is extremely important, as its existence has been connected to the thermodynamic features of the system, particularly to the WL. Indeed, FSC has been found to happen at the crossing of the WL both by computer simulations and experiments [20, 37–39, 41, 44]. Several water potentials, such as ST2 and TIP5P show FSC in correspondence to the WL [20]. Moreover, it has been shown that FSC occurs at the WL in TIP4P [27] and TIP4P/2005 bulk water [33]. A similar phenomenon has been observed in confined water [31, 32, 45] and in aqueous solutions [28] as well. From an experimental point of view, measurements made on water confined in nanoporous materials have shown a connection between FSC and a peak of the specific heat [40].

This evidence of the relation between the WL and FSC reveals a clear indication of a strong connection of dynamics and thermodynamics in supercooled water, and motivates the further analysis of this aspect of the liquid.

In the present paper, we review results from molecular dynamics (MD) simulations of supercooled water, from bulk water to aqueous solution and hydration water, where the relation between FSC and the WL is evident, demonstrating that this phenomenon is transversal and independent of the particular water potential. The paper is structured as follows: in Section 2 the details of the simulations used in this work are presented. Section 3 describes FSC in several systems analyzed by our group, from TIP4P and TIP4P/2005 bulk water, to SPC/E bulk and hydration water and TIP4P aqueous solution. In Section 4 a comparison of the locations of FSC and the WL between various potentials and systems is given. In Section 5 the conclusions are summarized.

2 Systems details

TIP4P bulk water. In the next section a review of results on TIP4P bulk water is presented, obtained by MD simulations in a series of papers [21, 27]. The TIP4P [46] geometry consists of three sites placed on the atomic positions. The hydrogen sites are charged, while the oxygen site is a neutral Lennard-Jones (LJ) site. The charge of the oxygen is placed on a fourth site, not coinciding with any of the atomic positions, along the H–O–H angle bisector, and coplanar with the oxygen and hydrogens atoms. Therefore globally, TIP4P is a rigid four-site model of water. The LLCP in TIP4P water is located at $T_c = 190$ K, $p_c = 150$ MPa and $\rho_c = 1.06$ g/cm^3 [21]. The densities investigated were $\rho = 0.95, 1.00, 1.03, 1.05, 1.10$ g/cm^3 from $T = 300$ K down to $T = 190$ K.

TIP4P/2005 bulk water. In the next sections, a review of results on TIP4P/2005 bulk water obtained in Ref. [33] by MD simulations is given. The TIP4P/2005 [47] is a reparametrization of the TIP4P model of water that keeps the geometry of the water molecule unchanged and yields to several improvements. The LLCP in TIP4P/2005 water is located at $T_c = 193$ K, $p_c = 135$

MPa and $\rho_c = 1.012$ g/cm^3 [22]. Cubic simulation boxes of 512 water molecules modeled with the TIP4P/2005 potentials were simulated at four different densities $\rho = 0.95, 0.98, 1.00, 1.03$ g/cm^3. The temperatures investigated were in a range from 300 K to 195 K.

SPC/E bulk water and protein hydration water. In the next sections, a review of results on SPC/E bulk water and SPC/E hydration water obtained in Ref. [48] by MD simulations is given. The SPC/E [49] is a rigid three-site model of water, consisting of three fixed charged sites on the atomic positions, and one LJ site coinciding with the oxygen position. A cubic simulation box containing 500 water molecules modeled with this potential was simulated along the $p = 1$ bar isobar in the 300 K−200 K temperature range. The results of hydration water were obtained for a system containing one lysozyme protein modeled by CHARMM [50, 51] force fields, and 13982 water molecules modeled with the SPC/E potential. The box also contained eight Cl^- counter ions to neutralize the charged lysozyme residues. The temperatures investigated in this system were ranging from 300 K to 200 K at a constant pressure of $p = 1$ bar. Hydration water is defined as water molecules lying at a distance less than or equal to 6 Å from any protein atoms.

The LLCP in SPC/E water is estimated at $T_c = 130$ K, $p_c = 290$ MPa, and $\rho_c = 1.10$ g/cm^3 [52]; consequently, the isobaric path simulated for bulk water should lie in the one-phase region below the critical point.

TIP4P aqueous solutions. In the next sections, a review of the results on NaCl water solution at a concentration $c = 0.67$ mol/kg obtained in a series of papers [21, 28, 53, 54] is given. Both water molecules and ions were described by using a combination of Coulombic and Lennard-Jones potentials. Water–water interaction parameters were those of the TIP4P [55] model and ion–ion interaction parameters were taken from Jensen and Jorgensen [56]; cross interaction parameters were calculated by using geometric mixing rules. These simulations were performed with a fixed number of 500 water molecules, six Na^+, and six Cl^-, along constant density paths at temperatures ranging from 300 K to 190 K. The LLCP from this solution is located at $T_c = 200$ K, $p_c = -50$ MPa and $\rho_c = 0.99$ g/cm^3 thus, its position moves to higher temperatures and lower pressures compared to those of bulk water [21]. The densities studied were $\rho = 0.92, 0.95, 0.97, 0.98, 1.05$ g/cm^3, where the latter density path lies above the LLCP.

3 Fragile to strong transition

Supercooled water dynamics was shown to be well described by the MCT, both from a computational and experimental viewpoint. In particular, its structural relaxation time τ increases as a power law well fitted by the following Equation predicted by MCT:

$$\tau \sim (T - T_C)^{-\gamma}, \tag{1}$$

where T_C is the Mode Coupling Temperature and γ the power law exponent. Equation 1 shows clearly that τ asymptotically diverges at T_C. At this temperature, the ideal version of MCT predicts an ideal phase transition of the liquid from an ergodic phase, where the system is able to structurally rearrange to a non- ergodic phase where the dynamics is completely arrested and the liquid becomes a glass.

Although the range of validity of MCT is wide, by further cooling, the progressive appearance of activated processes not taken into account by the ideal MCT, called hopping processes, allows the system to relax through a mechanism different from the cage breaking predicted by MCT, and it restores the ergodicity to the system also below T_C. The relaxation of the liquid also through hopping phenomena causes a crossover of the relaxation time increase, from the fragile MCT power law behavior to a strong Arrhenius exponential law:

$$\tau = \tau_0 e^{E_A/(k_B T)}, \tag{2}$$

where E_A is the activation energy. The FSC represents the transition of the system from a region where the relaxation mechanism is dominated by Brownian diffusion of the particles after the relaxation of the cages formed at intermediate times, to a region where the cages are almost completely frozen and particles escape from them by hopping processes. As it is shown in the following Sections the FSC in water is not only a dynamical phenomenon, but it is strongly related to the peculiar thermodynamic features of supercooled water.

3.1 TIP4P bulk water

To study the dynamical behavior of TIP4P bulk water and the eventual occurrence of FSC, MD simulations were performed on a cubic box of 512 molecules at different densities of $\rho = 0.95$, 1.00, 1.03, 1.05, and 1.10 g/cm^3 in temperature ranges from $T = 300$ K to $T = 190$ K [27]. For all the densities and temperatures investigated, the self-intermediate scattering functions (SISF) were calculated, showing a two-step relaxation scenario predicted by MCT [26]. The SISF are well fitted by the equation [23, 24]:

$$F_S(Q,t) = [1 - A(Q)]e^{-(t/\tau_s)^2} + A(Q)e^{-(t/\tau)^\beta}, \tag{3}$$

where $A(Q)$ is the Lamb–Mossbauer factor, τ_s the fast relaxation time, τ the long α-relaxation time and β the exponent of the stretched exponential describing the α-relaxation. As an example, Fig. 1 shows the oxygen

$F_S(Q,t)$ for TIP4P bulk water in the high-temperature and low-temperature regimes. At high T, the behavior of $F_S(Q,t)$ is that of a normal liquid and after the initial ballistic behavior, the particle changes to a diffusive behavior. For low temperatures, the correlator develops a plateau due to the transient caging of the nearest neighbors molecules. When the cages relax, the correlator decays in a stretched exponential fashion.

The results of the fits with Eq. (3) for the temperatures and densities analyzed show a progressive increasing of τ upon cooling the system. In Fig. 2 the α-relaxation time as a function of inverse temperature is plotted for three selected densities $\rho = 0.95$, 1.00, and 1.10 g/cm^3. For all densities the α-relaxation time increases with decreasing temperature. This trend indicates that upon lowering the temperature, liquid dynamics gradually becomes slower and the capability of the system to structurally rearrange decreases. Moreover, as a consequence of the diffusion anomaly of water, τ isothermally increases with the decreasing density. Lower densities, indeed, correspond to more locally ordered structures, and with less mobility compared to higher densities.

The solid and dashed lines in Fig. 2 are results from the fits with the power law of Eq. (1) and the exponential law of Eq. (2), respectively. Figure 2 shows that the data are well fitted by the MCT power law in the high-temperature range. Consequently, for all densities investigated, the dependence of τ on temperature in the mild supercooled regime follows the fragile behavior predicted by MCT. Upon cooling the system, deviations from this trend can be observed for all densities except for the highest $\rho = 1.10$ g/cm^3, and the low temperature behavior of the α-relaxation time is well fitted by the exponential Arrhenius law of Eq. (2). This deviation implies the existence of FSC from the high-temperature regime, where the system behaves as a fragile liquid, toward a deep supercooled regime where the system has a strong character. It is evident from Fig. 2, that the structural relaxation time increases as a power law with decreasing temperature only for $\rho = 1.10$ g/cm^3 in the whole range of temperatures simulated. The values of temperatures and densities of FSC (see Ref. [27]) have been compared with the values at which the isochoric specific heat c_V has a maximum, along each isochore. This line of c_V maxima is reasonably assumed to be a proxy for the WL. The calculation of c_V for all the state points investigated reveals the presence of a single maximum for all the densities studied except for $\rho = 1.10$ g/cm^3. The temperatures at which the maxima occur coincide with the FSC temperatures. This result is a convincing evidence of a strong connection between dynamics and thermodynamics in supercooled bulk water, and it is discussed in detail in Section 4.

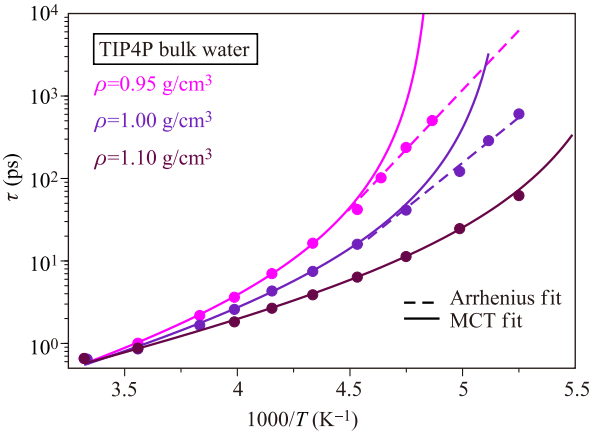

Fig. 2 α-relaxation time as a function of inverse temperature for $\rho = 0.95$, 1.00, and 1.10 g/cm^3 in the range of temperature investigated. The solid lines correspond to the MCT fits with the power law of Eq. (1) and the dashed lines correspond to the Arrhenius exponential fit of Eq. (2). Data from Ref. [27].

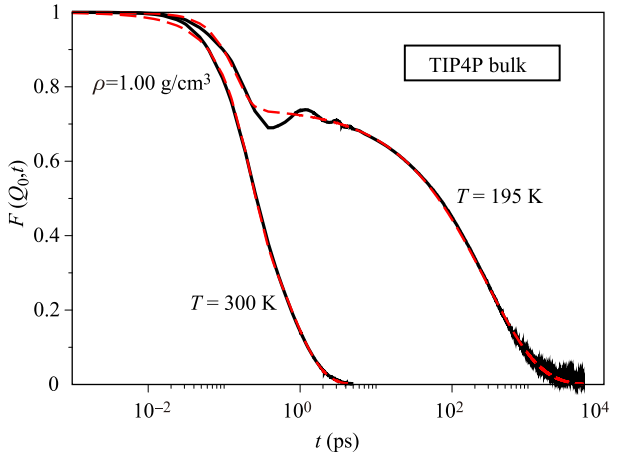

Fig. 1 Oxygen self-intermediate scattering functions (SISF) of TIP4P bulk water calculated at the maximum value Q_0 of the static structure factor for the density of $\rho = 1.00$ g/cm^3 in the high ($T = 300$ K) and low (195 K) temperature regimes. Data from Ref. [27].

3.2 TIP4P/2005 bulk water

Following the same line of the previous Section, the dynamical behavior of supercooled bulk water has been also studied for the widely used water potential, TIP4P/2005. In particular, MD simulations were performed on a cubic box of 512 molecules in the mild and deep supercooled regime, for four different densities, $\rho = 0.95$ g/cm^3, $\rho = 0.98$ g/cm^3, $\rho = 1.00$ g/cm^3, and $\rho = 1.03$ g/cm^3. For all densities investigated, SISF were computed and fitted with Eq. (3). As in the case of TIP4P, SISF are well fitted by Eq. (3) and exhibit a fast β-relaxation and

a slow α-relaxation, together with an intermediate cage regime [33]. The α-relaxation times for all the simulated state points have been calculated and plotted in Fig. 3 as a function of the inverse temperature for three selected densities $\rho = 0.95$ g/cm^3, $\rho = 0.98$ g/cm^3, and $\rho = 1.03$ g/cm^3. As shown Fig. 3, the relaxation time τ increases on decreasing the density. This behavior reflects the diffusion anomaly of water. In the mild supercooled regime, the relaxation time, for all densities investigated, increases following the MCT power law of Eq. (1) (solid lines in the Fig. 3) and, consequently, the system exhibits a fragile character of the relaxation process. In the low-temperature region and for all densities below the critical density $\rho = 1.012$ g/cm^3, a crossover from the fragile MCT power law to the Arrhenius exponential law of Eq. (2) (dashed lines in Fig. 3) occurs. As in the case of TIP4P and also for TIP4P/2005 the FSC points out the transition of the system from a fragile regime, where the liquid relaxes only structurally to a region where the relaxation process is more difficult to be carried out and hopping intervenes.

The dynamical aspects analyzed through the study of SISF in supercooled TIP4P/2005 water, were compared with the thermodynamic phase diagram in the same range of temperatures and densities. In particular, the isochoric specific heat c_V was calculated, and it was observed that all densities except $\rho = 1.03$ g/cm^3 it exhibit a single maximum. Importantly, each maximum occurs at values of temperature and density coincident with the location of the FSC, evidencing an underlying relation between dynamics and thermodynamics. This feature is examined in more detail in Section 4.

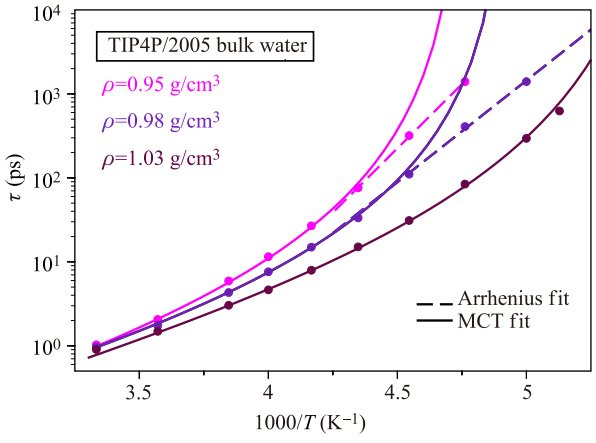

Fig. 3 α-relaxation time as a function of inverse temperature for $\rho = 0.95$, 0.98, and 1.03 g/cm^3 in the temperature range investigated. The solid lines correspond to the MCT fits with the power law of Eq. (1) and the dashed lines correspond to the Arrhenius exponential fit of Eq. (2). Data from Ref. [33].

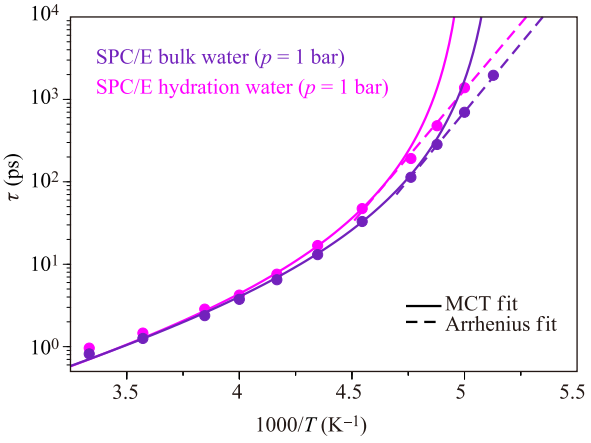

Fig. 4 α-relaxation times of bulk and hydration water as a function of inverse temperature. Solid lines are MCT fits via Eq. (1), and dashed lines are Arrhenius fits via Eq. (2). Data from Ref. [48].

3.3 SPC/E bulk and protein hydration water

This subsection deals with the α-relaxation of water simulated with the SPC/E potential. The dynamical behavior of bulk water and hydration water was characterized by the calculation of the density-density correlation functions. SISF of bulk water are well described by the model of Eq. (3). It was shown that SISF of hydration water cannot be described by the same model because of the coupling with the biomolecule, which causes the onset of a second, slower relaxational phenomenon called *long* [48, 57, 58]. In this case, the model has to be modified as follows:

$$F(q,t) = (1 - f_\alpha - f_{long})\mathrm{e}^{-(t/\tau_s)^2} + f_\alpha \mathrm{e}^{-(t/\tau_\alpha)^{\beta_\alpha}} + f_{long}\mathrm{e}^{-(t/\tau_{long})^{\beta_{long}}}, \quad (4)$$

where the added stretched exponential function describes the new, long relaxation. This relaxation occurs over a longer and well separated time scale with respect to the α-process; by fitting hydration water SISF via Eq. (4), it is possible to extract both τ_α and τ_{long}. Relaxation time τ_{long} is due to the coupling of water with the protein motion and it is not analyzed in this paper (see Ref. [48] for a detailed analysis).

The extracted α-relaxation times, τ_α of both bulk water and hydration water are shown in Fig. 4. At a given temperature the α-process of hydration water is slower compared to bulk water; the slowing down is more evident at low temperature. The temperature behavior upon cooling is similar: the α-relaxation times of both bulk and hydration water show a fragile to strong crossover. In protein hydration water, this occurs five degrees higher than in bulk water. The FSC in bulk water is also accompanied by a maximum in the constant pressure specific heat c_p, calculated along the simulated

isobar. This point is discussed in Section 4.

3.4 TIP4P aqueous solutions

Here, a review of the results for a NaCl water solution at concentration $c = 0.67$ mol/kg [28] is given. For studying the dynamical behavior of the water contained in electrolyte solutions, oxygen-oxygen SISF were calculated for different density values as a function of temperature. Structural α-relaxation times of water were then extracted from the fit via Eq. (3) of the self-density auto-correlation functions in the (Q, t) space. They are shown as a function of inverse temperature for three selected densities $\rho = 0.92$, 0.97, 1.05 g/cm^3 in Fig. 5. The behavior of the dynamics upon varying the density of the system is similar to that of bulk water: at fixed temperature, the dynamics is slower at a lower density. For each density, the MCT power law of Eq. (1) well describes the temperature dependence of τ_α upon cooling; however, the fit via Eq. (1) can only be done by excluding the lower temperature points at $\rho = 0.92$ g/cm^3 and $\rho = 0.97$ g/cm^3. Along these two isodensity paths, the relaxation times deviate from the MCT law upon cooling toward the Arrhenius law of Eq. (2). A FSC actually occurs along all density paths investigated in Ref. [28] and its crossover temperature coincides with the temperature of the maximum of the constant volume specific heat c_V, along the considered path calculated in Ref. [21]. The only exception to this phenomenology is the path corresponding to the highest density value $\rho = 1.05$ g/cm^3, which can be described by the MCT power law for the whole simulated temperature range, as shown in Fig. 5, similar to the results in the bulk phases of TIP4P and TIP4P/2005 water for the highest densities. We note

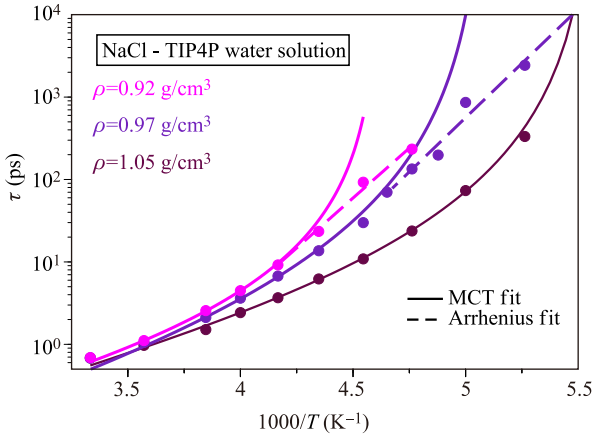

Fig. 5 α-relaxation time of the water contained in NaCl solutions as a function of inverse temperature. Solid lines are the MCT fits via Eq. (1), and dashed lines are the Arrhenius fits via Eq. (2). Data from Ref. [28].

that along $\rho = 1.05$ g/cm^3, no maximum in c_V was observed. This phenomenon is discussed in the next section, together with the same phenomenon observed in bulk TIP4P and TIP4P/2005 water.

4 FSC and Widom line

Figure 6 shows the location of FSC, the maxima of the specific heat and the LLCP for all systems analyzed in this paper. From Figure 6, it is evident that TIP4P and TIP4P/2005 bulk water have similar behaviors in the mild and deep supercooled regime. Indeed, for both potentials, FSC occurs in the same region of the phase diagram. Considering the location of the Widom line at the maxima of the specific heat, it can be seen that the two lines, the WL and FSC line, coincide. This result implies that, even if the phase diagrams of these two potentials are strongly different in the high temperature range, these differences tend to disappear upon supercooling.

For the same pressure, FSC for SPC/E bulk water is located at a lower temperature compared to that of TIP4P and TIP4P/2005, transition of the liquid from a fragile-like state, where it is more fluid and dynamically faster, toward a strong-like phase, where the liquid has a lower capability of rearrangement, happens later upon supercooling. This is consistent with the fact that the LLCP for SPC/E water is supposedly located at a lower temperature compared to TIP4P and TIP4P/2005. Furthermore, for this potential the occurrence of FSC and WL, calculated from the peak of the isobaric specific heat, coincides. From the position of FSC for SPC/E protein hydration water it can also be seen that the interactions of SPC/E hydration water with the lysozyme have the effect of isobarically translating FSC at higher temperature.

Finally, it can be seen in Fig. 6 that the location of FSC and the peaks of the specific heat for NaCl water solutions lie in a temperature and pressure range which is significantly different than that of bulk and hydration water. However, also in aqueous solutions, water exhibits a correspondence between dynamical FSC and the peaks of the isochoric specific heat, used as a proxy for the WL. Structural studies confirm this picture [54].

Overall, the analysis shows that the interconnection between FSC and the WL appears to be a universal phenomenon, independent of the particular geometry of the water potential, and not influenced by interactions with surfaces or ions. This result is extremely important as it proves the existence of a relation between the thermodynamic and dynamic properties of supercooled water. This connection can be interpreted in terms of phase diagram features for water in the supercooled regime. As

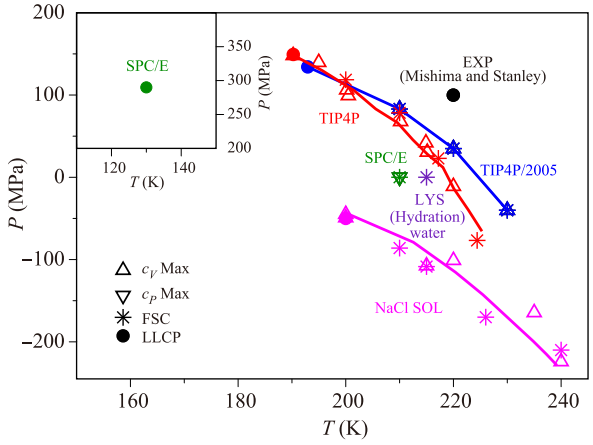

Fig. 6 Location of FSC (star), c_V maxima (triangle up), c_P maxima (triangle down), and LLCP (solid circle) in the P–T plane for TIP4P bulk water [21, 27] (red symbols), TIP4P/2005 bulk water [22, 23] (blue symbols), SPC/E bulk water [48, 52] (green symbols), SPC/E hydration water [48] (purple symbol) and NaCl aqueous solution [21, 28] (magenta symbols). The experimental LLCP is the estimated value in Refs. [12, 15]. The LLCP for SPC/E bulk water estimated in Ref. [52] is shown in the inset of the figure. The maximum error bars for the temperatures of the maxima of specific heat and FSC temperatures are estimated as 10 K and 5 K, respectively.

already mentioned, the WL marks the transition between a high-temperature HDL-like region, where water has greater mobility to a LDL-like state where the dynamics is slower and more frozen. Correspondingly, water changes from a phase where the relaxation mechanism is dominated by cage breaking and dynamics is more fragile-like, to a region where the system is more structurally arrested and relaxation happens through hopping processes, leading to a dynamical strong-like behavior.

5 Summary and conclusions

In this review, the dynamical and thermodynamic properties of supercooled water are considered. In TIP4P and TIP4P/2005 models of water, for which the position of the liquid–liquid critical point can be determined precisely, a comprehensive analysis of dynamical properties such as structural relaxation times and thermodynamic properties for pressures above and below the critical point can be performed. For water, modeled with these two potentials, the fragile to strong crossover of α-relaxation times at $p < p_c$ coincides with the crossing of the Widom line. Above the liquid–liquid critical point pressure, no maxima of the response functions are observed, and no fragile to strong crossovers of α-relaxation times occur. The latter point is valid at least down to the lowest temperature investigated upon cooling at $p > p_c$ and $\rho > \rho_c$. It should be emphasized that those paths were all within the high-density phase of supercooled water, and therefore, they did not cross either the coexistence line or the mechanical stability limit line of the high-density liquid.

In electrolyte aqueous solutions at $c = 0.67$ mol/kg, the water phenomenology is qualitatively unaffected by the presence of ions. The existence of the liquid–liquid critical point, and consequently, the Widom line is preserved in these conditions. The net effect on the complex thermodynamic behavior of water can be seen as a shift toward lower pressures and higher temperatures by a similar phenomenology of the fragile to strong crossover above and below the critical point pressure.

For SPC/E bulk water, the fragile to strong crossover of α-relaxation times along the $p = 1$ bar isobar occurs at the same temperature at which the thermodynamic response function shows a maximum. This behavior is expected in the one-phase region $p < p_c$, in analogy to the other investigated systems, and also in accordance to free-energy based calculations for the position of the liquid–liquid critical point in this model of water [52]. Upon cooling, hydration water exhibits a fragile to strong crossover in its α-relaxation time as well, but the thermodynamic response function cannot be calculated directly for this system. However, the strong evidence provided by other systems leaves the possibility open that a Widom line can also exist in hydration water, and consequently, a transformation between high density and low density in the structure of the water belonging to the closest layers of proteins. The occurrence of the fragile to strong crossover at the maximum of the specific heat has been observed only in the mono-layer water surrounding the hydrated powder model of lysozyme proteins [59, 60].

As a summary, the fragile to strong crossover, which can be measured in experiments probing translational dynamics, represents the *smoking gun* for the existence of a liquid–liquid critical point in water, not only in the bulk phase but also in solution, where supercooling is easier to obtain.

References

1. P. Gallo, K. Amann-Winkel, C. A. Angell, M. A. Anisimov, F. Caupin, C. Chakravarty, E. Lascaris, T. Loerting, A. Z. Panagiotopoulos, J. Russo, J. A. Sellberg, H. E. Stanley, H. Tanaka, C. Vega, L. Xu, and G. M. P. Lars, Water: A tale of two liquids, *Chem. Rev.* 116(13), 7463 (2016)
2. P. Ball, Water - An enduring mystery, *Nature* 452(7185), 291 (2008)
3. P. G. Debenedetti, Supercooled and glassy water, *J. Phys.: Condens. Matter* 15(45), R1669 (2003)

4. C. A. Angell, R. D. Bressel, M. Hemmati, E. J. Sare, and J. C. Tucker, Water and its anomalies in perspective: Tetrahedral liquids with and without liquid-liquid phase transitions, *Phys. Chem. Chem. Phys.* 2(8), 1559 (2000)
5. P. G. Debenedetti, Metastable Liquids: Concepts and Principles, Princeton: Princeton University Press, 1996
6. A. Sakai, T. Matsumoto, D. Hirai, and T. Niino, Newly developed encapsulation-dehydration protocol for plantcryopreservation, *Cryo Lett.* 21(1), 53 (1999)
7. W. Kauzmann, Some factors in the interpretation of protein denaturation, *Adv. Protein Chem.* 14, 1 (1959)
8. F. Franks, Water: A Matrix of Life, RSC Paperbacks, 2nd edition, Cambridge, UK: The Royal Society of Chemistry, 2000
9. P. G. Debenedetti and H. E. Stanley, Supercooled and glassy water, *Phys. Today* 56(6), 40 (2003)
10. C. A. Angell, J. Shuppert, and J. C. Tucker, Anomalous properties of supercooled water. Heat capacity, expansivity, and proton magnetic resonance chemical shift from 0 to −38%, *J. Phys. Chem.* 77(26), 3092 (1973)
11. R. J. Speedy and C. A. Angell, Isothermal compressibility of supercooled water and evidence for a thermodynamic singularity at −45°C, *J. Chem. Phys.* 65(3), 851 (1976)
12. O. Mishima and H. E. Stanley, The relationship between liquid, supercooled and glassy water, *Nature* 396(6709), 329 (1998)
13. P. H. Poole, F. Sciortino, U. Essmann, and H. E. Stanley, Phase behaviour of metastable water, *Nature* 360(6402), 324 (1992)
14. K. Winkel, M. S. Elsaesser, E. Mayer, and T. Loerting, Water polyamorphism: Reversibility and (dis) continuity, *J. Chem. Phys.* 128(4), 044510 (2008)
15. O. Mishima and H. E. Stanley, Decompression-induced melting of ice IV and the liquid-liquid transition in water, *Nature* 392(6672), 164 (1998)
16. O. Mishima, L. D. Calvert, and E. Whalley, An apparently first-order transition between two amorphous phases of ice induced by pressure, *Nature* 314(6006), 76 (1985)
17. K. Winkel, E. Mayer, and T. Loerting, Equilibrated high-density amorphous ice and its first-order transition to the low-density form, *J. Phys. Chem. B* 115(48), 14141 (2011)
18. C. U. Kim, B. Barstow, M. V. Tate, and S. M. Gruner, Evidence for liquid water during the high-density to low-density amorphous ice transition, *Proc. Natl. Acad. Sci. USA* 106(12), 4596 (2009)
19. G. Franzese and H. E. Stanley, The widom line of supercooled water, *J. Phys.: Condens. Matter* 19(20), 205126 (2007)
20. L. Xu, P. Kumar, S. V. Buldyrev, S. H. Chen, P. H. Poole, F. Sciortino, and H. E. Stanley, Relation between the Widom line and the dynamic crossover in systems with a liquid-liquid phase transition, *Proc. Natl. Acad. Sci. USA* 102(46), 16558 (2005)
21. D. Corradini, M. Rovere, and P. Gallo, A route to explain water anomalies from results on an aqueous solution of salt, *J. Chem. Phys.* 132(13), 134508 (2010)
22. J. L. F. Abascal and C. Vega, Widom line and the liquid-liquid critical point for the TIP4P/2005 water model, *J. Chem. Phys.* 133(23), 234502 (2010)
23. P. Gallo, F. Sciortino, P. Tartaglia, and S. H. Chen, Slow dynamics of water molecules in supercooled states, *Phys. Rev. Lett.* 76(15), 2730 (1996)
24. F. Sciortino, P. Gallo, P. Tartaglia, and S. H. Chen, Supercooled water and the kinetic glass transition, *Phys. Rev. E* 54(6), 6331 (1996)
25. W. Gotze and L. Sjogren, Relaxation processes in supercooled liquids, *Rep. Prog. Phys.* 55(3), 241 (1992)
26. W. Götze, Complex Dynamics of Glass-Forming Liquids: A Mode-Coupling Theory, Oxford: Oxford University Press, 2009
27. P. Gallo and M. Rovere, Mode coupling and fragile to strong transition in supercooled TIP4P water, *J. Chem. Phys.* 137(16), 164503 (2012)
28. P. Gallo, D. Corradini, and M. Rovere, Fragile to strong crossover at the Widom line in supercooled aqueous solutions of NaCl, *J. Chem. Phys.* 139(20), 204503 (2013)
29. P. Gallo, M. Rovere, and E. Spohr, Supercooled confined water and the mode coupling crossover temperature, *Phys. Rev. Lett.* 85(20), 4317 (2000)
30. P. Gallo, M. Rovere, and E. Spohr, Glass transition and layering effects in confined water: A computer simulation study, *J. Chem. Phys.* 113(24), 11324 (2000)
31. P. Gallo, M. Rovere, and S. H. Chen, Dynamic crossover in supercooled confined water: Understanding bulk properties through confinement, *J. Phys. Chem. Lett.* 1(4), 729 (2010)
32. P. Gallo, M. Rovere, and S. H. Chen, Water confined in MCM-41: A mode coupling theory analysis, *J. Phys.: Condens. Matter* 24(6), 064109 (2012)
33. M. De Marzio, G. Camisasca, M. Rovere, and P. Gallo, Mode coupling theory and fragile to strong transition in supercooled TIP4P/2005 water, *J. Chem. Phys.* 144(7), 074503 (2016)
34. A. Dehaoui, B. Issenmann, and F. Caupin, Viscosity of deeply supercooled water and its coupling to molecular diffusion, *Proc. Natl. Acad. Sci. USA* 112(39), 12020 (2015)
35. R. Torre, P. Bartolini, and R. Righini, Structural relaxation in supercooled water by time-resolved spectroscopy, *Nature* 428(6980), 296 (2004)
36. F. W. Starr, F. Sciortino, and H. E. Stanley, Dynamics of simulated water under pressure, *Phys. Rev. E* 60(6), 6757 (1999)
37. A. Faraone, L. Liu, C. Y. Mou, C. W. Yen, and S. H. Chen, Fragile-to- strong liquid transition in deeply supercooled confined water, *J. Chem. Phys.* 121(22), 10843 (2004)

38. L. Liu, S. H. Chen, A. Faraone, C. W. Yen, and C. Y. Mou, Pressure dependence of fragile-to-strong transition and a possible second critical point in supercooled confined water, *Phys. Rev. Lett.* 95(11), 117802 (2005)
39. F. Mallamace, M. Broccio, C. Corsaro, A. Faraone, U. Wanderlingh, L. Liu, C. Y. Mou, and S. H. Chen, The fragile-to-strong dynamic crossover transition in confined water: nuclear magnetic resonance results, *J. Chem. Phys.* 124(16), 161102 (2006)
40. Y. Zhang, M. Lagi, E. Fratini, P. Baglioni, E. Mamontov, and S. H. Chen, Dynamic susceptibility of supercooled water and its relation to the dynamic crossover phenomenon, *Phys. Rev. E* 79(4), 040201 (2009)
41. L. Liu, S. H. Chen, A. Faraone, C.W. Yen, C. Y. Mou, A. I. Kolesnikov, E. Mamontov, and J. Leao, Quasi-elastic and inelastic neutron scattering investigation of fragile-to-strong crossover in deeply supercooled water confined in nanoporous silica matrices, *J. Phys.: Condens. Matter* 18(36), S2261 (2006)
42. Z. Wang, P. Le, K. Ito, J. B. Leão, M. Tyagi, and S. H. Chen, Dynamic crossover in deeply cooled water confined in mcm-41 at 4 kbar and its relation to the liquid-liquid transition hypothesis, *J. Chem. Phys.* 143(11), 114508 (2015)
43. Y. Xu, N. G. Petrik, R. S. Smith, B. D. Kay, and G. A. Kimmel, Growth rate of crystalline ice and the diffusivity of supercooled water from 126 to 262 K, *Proc. Natl. Acad. Sci. USA* 113(52), 14921 (2016)
44. J. M. Zanotti, M. C. Bellissent-Funel, and S. H. Chen, Relaxational dynamics of supercooled water in porous glass, *Phys. Rev. E* 59(3), 3084 (1999)
45. P. Gallo, M. Rovere, and S. H. Chen, Anomalous dynamics of water confined in MCM-41 at different hydrations, *J. Phys.: Condens. Matter* 22(28), 284102 (2010)
46. W. L. Jorgensen, J. Chandrasekhar, J. D. Madura, R. W. Impey, and M. L. Klein, Comparison of simple potential functions for simulating liquid water, *J. Chem. Phys.* 79(2), 926 (1983)
47. J. L. F. Abascal and C. Vega, A general purpose model for the condensed phases of water: TIP4P/2005, *J. Chem. Phys.* 123(23), 234505 (2005)
48. G. Camisasca, M. De Marzio, D. Corradini, and P. Gallo, Two structural relaxations in protein hydration water and their dynamic crossovers, *J. Chem. Phys.* 145(4), 044503 (2016)
49. J. C. Herman, Berendsen, J. R. Grigera, and T. P. Straatsma. The missing term in effective pair potentials, *J. Phys. Chem.* 91(24), 6269 (1987)
50. A. D. MacKerell, D. Bashford, M. Bellott, R. L. Dunbrack, J. D. Evanseck, M. J. Field, S. Fischer, J. Gao, H. Guo, S. Ha, D. Joseph-McCarthy, L. Kuchnir, K. Kuczera, F. T. Lau, C. Mattos, S. Michnick, T. Ngo, D. T. Nguyen, B. Prodhom, W. E. Reiher, B. Roux, M. Schlenkrich, J. C. Smith, R. Stote, J. Straub, M. Watanabe, J. Wiórkiewicz-Kuczera, D. Yin, and M. Karplus, All-atom empirical potential for molecular modeling and dynamics studies of proteins, *J. Phys. Chem. B* 102(18), 3586 (1998)
51. A. D. MacKerell, M. Feig, and C. L. Brooks, Extending the treatment of backbone energetics in protein force fields: limitations of gas-phase quantum mechanics in reproducing protein conformational distributions in molecular dynamics simulations, *J. Comput. Chem.* 25(11), 1400 (2004)
52. A. Scala, F. W. Starr, E. La Nave, H. E. Stanley, and F. Sciortino, Free energy surface of supercooled water, *Phys. Rev. E* 62(6), 8016 (2000)
53. D. Corradini and P. Gallo, Liquid-liquid coexistence in nacl aqueous solutions: a simulation study of concentration effects, *J. Phys. Chem. B* 115, 1461 (2011)
54. D. Corradini, M. Rovere, and P. Gallo, Structural properties of high and low density water in a supercooled aqueous solution of salt, *J. Phys. Chem. B* 115(6), 1461 (2011)
55. C. Vega, J. L. F. Abascal, M. M. Conde, and J. L. Aragones, What ice can teach us about water interactions: A critical comparison of the performance of different water models, *Faraday Discuss.* 141, 251 (2009)
56. K. P. Jensen and W. L. Jorgensen, Halide, ammonium, and alkali metal ion parameters for modeling aqueous solutions, *J. Chem. Theory Comput.* 2(6), 1499 (2006)
57. A. Magno and P. Gallo, Understanding the Mechanisms of Bioprotection: A Comparative Study of Aqueous Solutions of Trehalose and Maltose upon Supercooling, *J. Phys. Chem. Lett.* 2(9), 977 (2011)
58. D. Corradini, E. G. Strekalova, H. E. Stanley, and P. Gallo, Microscopic mechanism of protein cryopreservation in an aqueous solution with trehalose, *Sci. Rep.* 3(1), 1218 (2013)
59. P. Kumar, Z. Yan, Limei Xu, M. G. Mazza, S. V. Buldyrev, S. H. Chen, S. Sastry, and H. E. Stanley, Glass transition in biomolecules and the liquid-liquid critical point of water, *Phys. Rev. Lett.* 97(17), 177802 (2006)
60. S. H. Chen, L. Liu, E. Fratini, P. Baglioni, A. Faraone, E. Mamontov, and M. Fomina, Observation of fragile-to-strong dynamic crossover in protein hydration water, *Proc. Natl. Acad. Sci. USA* 103(24), 9012 (2006)